*Structural Engineering and Mechanics, Vol.1, No.1 (1993) 17-30*
DOI: http://dx.doi.org/10.12989/sem.1993.1.1.017


# Multi-spring model for 3-dimensional analysis of RC members

Kang-Ning Li†

*Department of Civil Engineering, National University of Singapore, Singapore 0511*

Shunsuke Otani‡

*Department of Architecture, the University of Tokyo, Tokyo 113, Japan*

**Abstract.** A practical multi-spring model is proposed for a nonlinear analysis of reinforced concrete members, especially columns, taking into account the interaction of axial load and bi-directional bending moment. The parameters of the model are determined on the basis of material properties and section geometry. The axial force-moment interaction curve of reinforced concrete sections predicted by the model was shown to agree well with those obtained by the flexural analysis utilizing realistic stress-strain relations of materials. The reliability of the model was also examined with respect to the test of reinforced concrete columns subjected to varying axial load and bi-directional lateral load reversals. The analytical results agreed well with the experiment.

**Key words:** nonlinear analysis; reinforced concrete members; columns; multi-spring model; flexural deformation; varying-axial load; bi-directional moment interaction; axial load-moment interaction; axial deformation-rotation interaction.

## 1. Introduction

The moment-curvature analysis of a reinforced concrete (RC) "section" under load reversals is normally based on (a) an assumption, known as Bernoulli's hypothesis, that a plane section remains plane after deformation, (b) uni-axial stress-strain relations of materials and (c) equilibrium of forces (e.g., Kent and Park 1971). The deformation of a member may be calculated by a double integration of curvature with respect to member length; however, the deformation calculated underestimates that observed in a test (a) because the Bernoulli's hypothesis holds only in an approximate sense, and (b) because additional deformations caused by shear cracking and by the pull-out of longitudinal reinforcement from the anchorage are neglected. Therefore, in a nonlinear analysis of an RC building structure, many researchers simply assumed all the inelastic deformation to concentrate at the member ends (Giberson 1967) and used a member-end moment-rotation hysteresis relation. The method was shown to reasona-

† Research Scientist
‡ Associate Professor

bly simulate the response observed in a full-scale test of an RC building under lateral load reversals to failure (Otani et al. 1985).

## 2. Interaction of resistances and deformations

The flexural behavior of an RC column section is influenced by existing axial load; the phenomenon normally called as the interaction of axial force and bending moment. The interaction of axial deformation and curvature also exists; e.g., in an RC member under pure bending, the neutral axis of section shifts to compression side after cracking, which accompanies the elongation at the centroid of the section although no tensile force is applied; i.e., pure bending causes elongation of a member after cracking.

Furthermore, a column during a real earthquake motion is subjected to bi-directional shear and bending. The bending capacity in a principal direction is influenced by an existing bending moment in the orthogonal direction, the phenomenon called the bi-directional bending interaction. Takizawa and Aoyama (1976) used a plasticity theorem in constructing hysteresis relation under bi-directional bending interaction. Fukuzawa et al. (1988) extended the Takizawa's work to include the tri-axial interaction of varying axial load and bi-directional bending.

## 3. Multi-spring model

A multi-spring model was proposed by Lai et al. (1984) to simulate the flexural behavior of RC columns under varying axial load and bi-directional lateral load reversals. A column was idealized by an elastic element with two multi-spring elements of zero-length at the column ends (Fig.1); a multi-spring element consisted of 5 concrete and 4 steel longitudinal springs. Spring parameters were so defined to approximate the axial force-bending moment interaction curve at some selected axial force levels. This made the model difficult to use in the analysis. Moreover, the interaction curve of the model deviated from the interaction curve due to the use of fewer number of springs. Jiang and Saiidi (1990) proposed to combine the hysteresis properties of concrete and steel springs in a corner to simplify the model. Li et al.

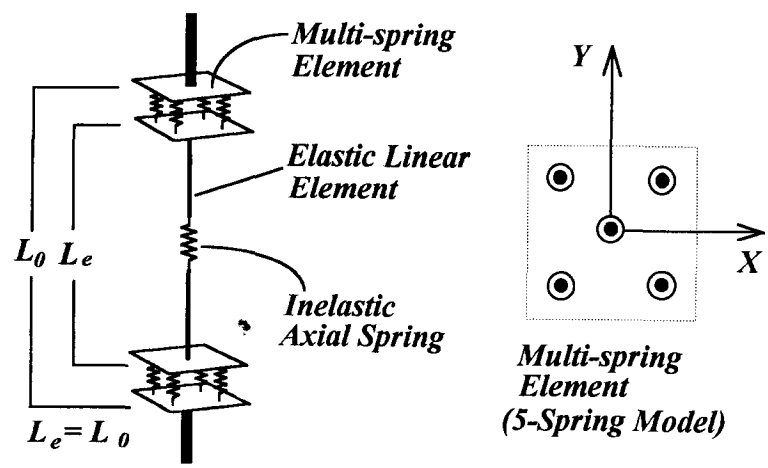


Fig. 1 Column Idealized by Multi-Spring Model

(1988) modified the hysteretic properties of concrete and steel springs, and demonstrated the reliability of the model against column test results.

In this paper, the number of springs in a multi-spring element is increased. Note that the simpler a model is, the more judgment is required to determine model properties. With an increase in the number of springs in a multi-spring element, the simulation capability of the interaction behavior is improved, and the determination of the stiffness properties of each spring is simplified. On the other hand, a nonlinear earthquake response analysis of a large three-dimensional frame under bi-directional earthquake excitation (Li et al., 1989) indicated that the total computation time did not increase significantly because (a) the yielding of columns takes place only at the base of first-story columns in a properly designed (weak-beam strong-column) building, and (b) the number of degrees of freedom of a spring element can be reduced to three (bi-directional rotations and axial elongation).

For a rectangular RC section, the use of 8 core concrete springs and 8 shell concrete springs (16-concrete spring model) is proposed as shown in Fig.2(a); a concrete spring is located at the centroid of a subdivided area. The stiffness properties of core and shell concrete springs are made different to consider the confining effect by lateral reinforcement. A steel spring may be located at a reinforcing bar; however, the spring may be placed at the center of multiple reinforcing bars; a typical example using 9 steel springs is shown in Fig.2(b). Thus the location of a spring is automatically determined without making use of an axial force-moment interaction curve of the section.

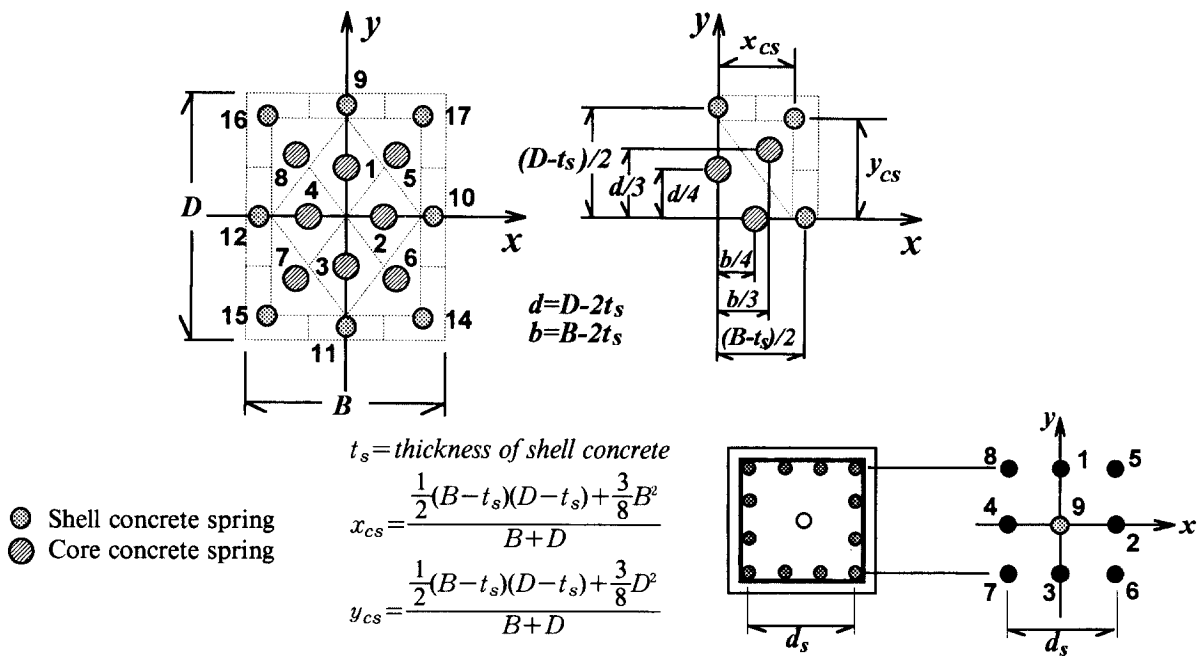


$$x_{cs}=\frac{\frac{1}{2}(B-t_s)(D-t_s)+\frac{3}{8}B^2}{B+D}$$

$$y_{cs}=\frac{\frac{1}{2}(B-t_s)(D-t_s)+\frac{3}{8}D^2}{B+D}$$

(a) 16-Concrete Spring (b) 9-Steel Spring

Fig. 2 Spring Elements for Rectangular Section

## 4. Stiffness properties of steel and concrete springs

The spring force is calculated as a product of the tributary area of the spring and a stress of the material at the centroid of the area. The Bernoulli's hypothesis was used to determine the deformation distribution in a multi-spring element. An imaginary spring length $\eta L_0$ expressing plastic zone is assumed to calculate the deformation for a given strain, although the multi-spring element was treated as zero-length. The plastic zone length was arbitrarily assumed to be one half the member depth $D$; it should be determined considering (a) the variation of strain within the plastic zone, (b) the deformation associated with concrete cracking beyond the plastic zone and (c) the deformation caused by the pull-out of reinforcement from the anchorage zone. A trilinear force-deformation relationship (Fig.3) is assumed for a steel spring and for a concrete spring under compression.

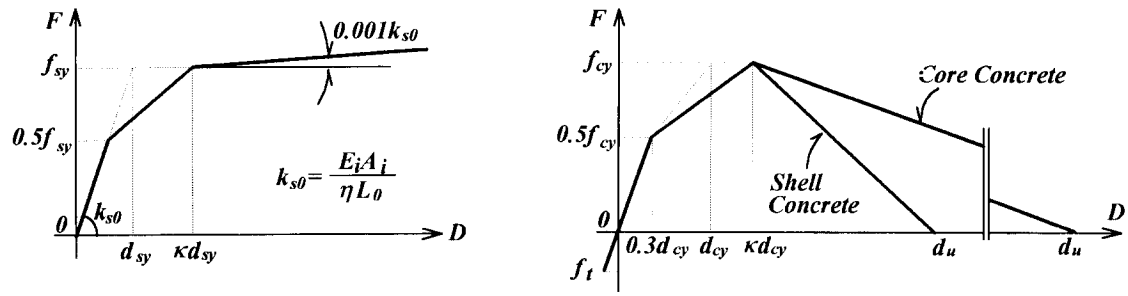


(a) Steel Spring (b) Concrete Spring

Fig. 3 Spring Force-Displacement Relationships

The flexural deformation in the middle part of a member increases with a shear-span-to-depth ratio, whereas the contribution of shear deformation decreases with the ratio. The amount of pull-out deformation may be calculated if the bond stress-slip relation is given. However, these additional deformations could not be defined by theoretical calculation at present. An empirical parameter $\kappa$ is introduced to approximate the additional deformations;

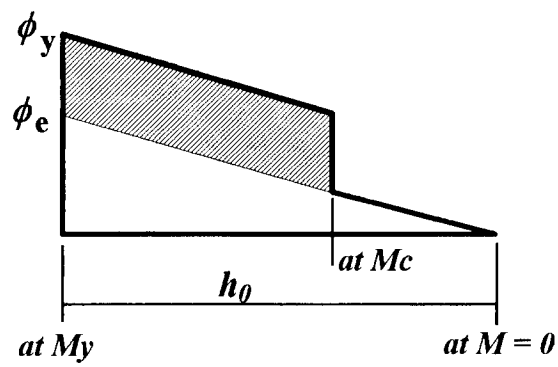


Fig. 4 Assumption of Curvature Distribution

$$\kappa = \begin{cases} 1.0 & (h_0/D \leq 1.0) \\ 1.0 + \dfrac{h_0/D - 1.0}{h_0/D} & (h_0/D > 1.0) \end{cases} \quad (1)$$

where, $h_0/D$=shear span-to-depth ratio of a member. Equation (1) was derived on the basis of column test data (Li, et al. 1985) and for a flexural curvature distribution as given in Fig.4. The same parameters of $\eta L_0$ and $\kappa$ are used for both steel and concrete springs.

*Concrete Spring*: The force-deformation relationship for a concrete spring is assumed identical for core and shell concrete until maximum resistance, $f_{cy}$, is attained at concrete compressive strength $\sigma_B$. The deformation at the maximum resistance is calculated to be $\kappa d_{cy}$, where $d_{cy} = \varepsilon_B \cdot \eta L_0$ ($\varepsilon_B$ is the strain at the strength $\sigma_B$). The elastic stiffness of the concrete spring was changed at resistance $0.5 f_{cy}$ and deformation $0.3 d_{cy}$ to approximate the stress-strain curve of concrete. The descending branch of the force-deformation relationship is made different for core and shell concrete taking the effect of confinement into consideration; i.e., the displacement $d_u$ at null resistance is defined as $d_u = \mu \kappa d_{cy}$, where, $\mu = \varepsilon_u / \varepsilon_B$. Note that $\varepsilon_u$ was calculated by the equations (Park et al. 1982) shown in Fig.5 for shell concrete and for core concrete allowing for confining effect. The same initial stiffness is assumed in tension.

*Steel Spring*: Displacement $d_{sy}$ of a steel spring is determined by yielding strain $\varepsilon_{sy}$ and the plastic zone length $\eta L_0$, i.e., $d_{sy} = \varepsilon_{sy} \cdot \eta L_0$. The yielding resistance of steel spring develops at the displacement of $\kappa d_{sy}$. The elastic stiffness is changed at $0.5 f_{sy}$. A finite stiffness is assumed after yielding for the purpose of stabilizing the numerical computation rather than for the effect of strain hardening. The force-deformation relation of a steel spring is symmetric in tension and compression.

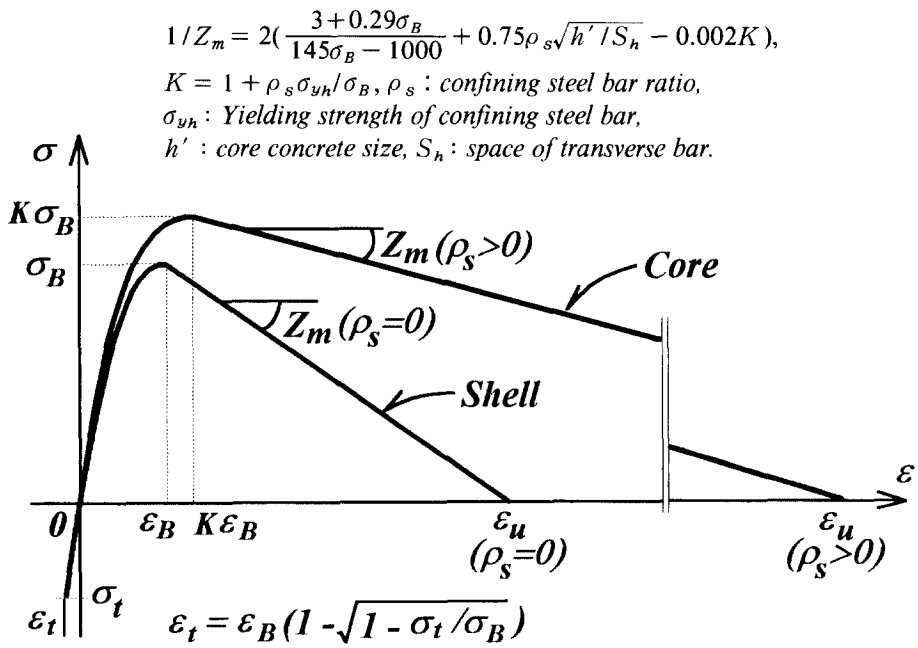


Fig. 5 Concrete Stress-Strain Curves

## 5. Stiffness of elastic element

The total bending flexibility of a simply supported member under uni-directional bending moment at the two ends can be expressed as

$$\begin{bmatrix} \frac{L_0}{3EI} & \frac{-L_0}{6EI} \\ \frac{-L_0}{6EI} & \frac{L_0}{3EI} \end{bmatrix} = \begin{bmatrix} \frac{\gamma_m L_0}{3EI} + \delta_m & \frac{-L_0}{6EI} \\ \frac{-L_0}{6EI} & \frac{\gamma_m L_0}{3EI} + \delta_m \end{bmatrix} \tag{2}$$

where, $E$=Young's modulus, $I$=inertia moment of the section, $L_0$=the length of elastic element, $\gamma_m$= a reduction factor for the initial flexibility of elastic element. $\delta_m$ = the initial flexibility of multi-spring element. The factor $\gamma_m$ was introduced to account for the initial flexibility $\delta_m$ of the multi-spring elements. $\delta_m$ can be expressed as

$$\delta_m = \frac{\eta L_0}{\sum E_i A_i Y_i^2} \approx \frac{\eta L_0}{0.9EI} \tag{3}$$

where, $E_i A_i$ =i-th spring stiffness, $Y_i$ =i-th spring location. The moment of inertia of a multi-spring model is approximately $0.9I$ ($I=BD^3/12$) for a rectangular member section with 16 concrete springs. Hence, the reduction factor $\gamma_m$ can be calculated as

$$\gamma_m = 1.0 - \eta/0.3 \tag{4}$$

Similarly, a reduction factor $\gamma_0 = 1.0 - 2\eta$ is used for the initial axial flexibility of the elastic element. Inelastic stiffness can be used for the axial and shear stiffness of the elastic element.

## 6. Examination of the multi-spring model

An earthquake response of a structure is sensitive to the lateral resistance; hence, it is important to accurately estimate the resistance of constituent members. The reliability of the multi-spring model is studied about axial load-moment interaction curves. Three RC sections are used for the examination; Sections S1 to S3. The geometry of the sections is shown in Fig. 6. Note that Section S3 is not symmetric.

The stress-strain relation is assumed to be elastic-perfectly plastic for the steel, and that for concrete is shown in Fig.5 for confined and shell concrete. The material properties and model parameters are listed in Tables 1 and 2. The confining factor $K$ was assumed for each section as listed in Table 1. For the proposed model, 9 steel springs are used for Sections S1 and S2, and the area of reinforcing bars not at the spring location is distributed to 4 middle springs by linear interpolation. Steel springs are assigned at each reinforcing bar for Section S3. Relative values of $d_{cy}$, $d_{sy}$ of concrete and steel spring deformation ($d_{cy}/d_{sy} = \varepsilon_B/\varepsilon_{sy}$) are used in the calculation. The parameters of the original multi-spring model with 5-spring are determined for an axial force-bending moment interaction curve at axial load level equal to $0.2BD\sigma_B$. The $N$-$M_x$-$M_y$ curves by integration method are calculated using the Bernoulli's hypothesis, stress-strain relations of the materials, and equilibrium of forces. Concrete tensile strength is considered in calculating cracking moment. A yield moment is calculated for the first yielding of a reinforcing bar.

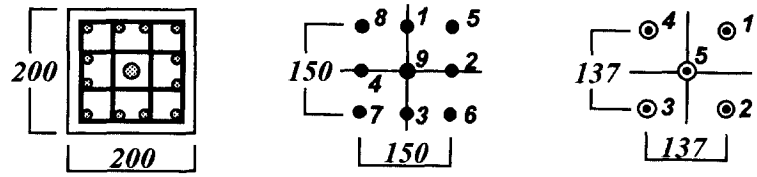


12-D10, D25 9-Steel Spring Original Model

(a) $S1(b=d=160, t_s=20)$

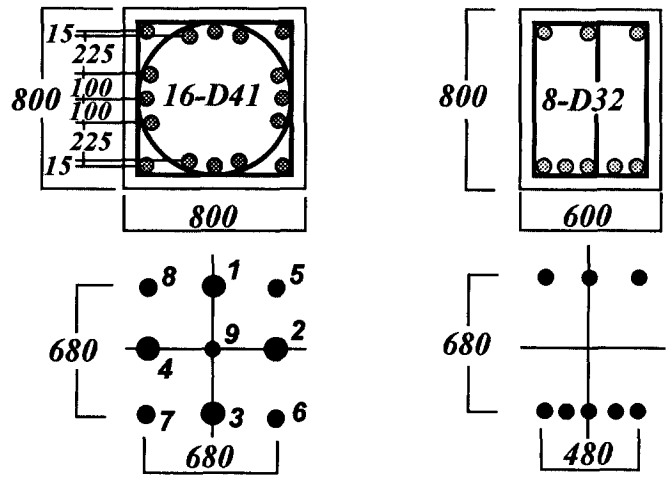


9-Steel Spring 8-Steel Spring

(b) $S2$ (c) $S3$

$(b=d=700, t_s=50)$ $(b=480, d=680, t_s=60)$

Fig. 6 RC Column Sections $S1$ to $S3$(Unit in mm)

Table 1 Material Properties of Sections S1 to S3

| Section | | S1 | | S2, S3 | |
|---|---|---|---|---|---|
| Steel Bar | Type | D10 | D25 | D32 | D41 |
| | Area($mm^2$) | 71 | 507 | 794 | 1340 |
| | $\sigma_{sy}$(MPa) | 324 | 362 | 417 | 417 |
| | $E_s$($10^5$MPa) | 1.87 | 1.81 | 2.1 | 2.1 |
| Concrete | $K$ | 1.25 | | 1.2 | |
| | $\sigma_B$(MPa) | 27.5 | | 30.7 | |
| | $\varepsilon_B$ | 0.002 | | 0.0022 | |
| | $\sigma_t$(MPa) | 2.6 | | 2.65 | |

Table 2 Multi-Spring Parameters for Sections S1 to S3

| | Model | Steel Spring No.: $f_{sy}$(kN) | Concrete Spring No.: $f_{cy}$(kN) |
|---|---|---|---|
| S1 | 5-SS, 5-CS* | 1~4:69.2; 5:184 | 1~4:218; 5:316 |
| | 9-SS, 16-CS | 1~4:30.8; 5~8:38.5; 9:184 | 1~8:110; 9~12:44; 13~16:55 |
| S2 | 9-SS, 16-CS | 1~4:874; 5~8:1330; 9:136 | 1~8:2260; 9~12:54; 13~16:62 |
| S3 | 8-SS, 16-CS | 1~8:331 | 1~8:1510; 9:442; 10:626; 11;442; 12:626; 13~16:645 |

* SS: Steel Spring; CS: Concrete Spring

The interaction curves of bi-directional maximum bending moments are calculated for Section S1 at different axial load levels; i.e., a maximum bending moment is calculated under a constant axial force and monotonically increasing curvature in a given direction. The axial force is normalized by the sectional area and concrete compressive strength, and called an axial stress ratio. The curves calculated by the original multi-spring model and the proposed model are compared with the exact curves in Fig.7, in which the curves are shown separately

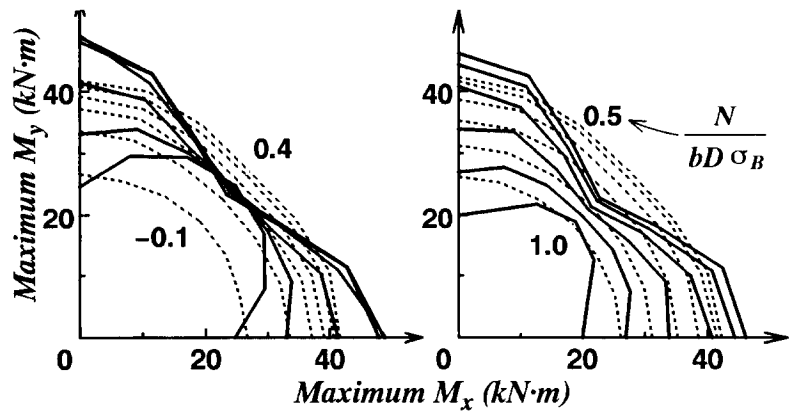


(a) Original Model with 5-Spring

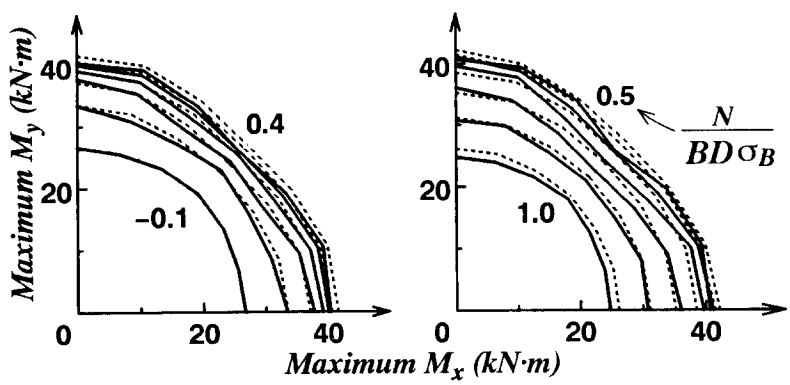


(b) Proposed Model(9-SS, 16-CS)

Fig. 7 Comparison of $N$-$M_x$-$M_y$ Curves of Section S1 by Models (Solid) and Integration Method(Dash)

for compression failure and tensile failure zones (axial stress ratios above 0.5 and below 0.4). The original model using only five concrete springs does not favorably simulate the exact interaction curves, particularly in a 45-degree diagonal direction from a principal axis of the section. In contrast, the proposed model with 9-steel and 16-concrete springs showed a satisfactory agreement with the exact analysis.

Axial force-bending moment interaction curves of Section S2 and S3 are calculated and shown in Fig.8. The moments of cracking $M_c$, yielding $M_y$ and ultimate $M_{max}$ are under loading in a 45-degree direction from a principal section axis. The curves by the proposed model agree favorably with the exact curves.

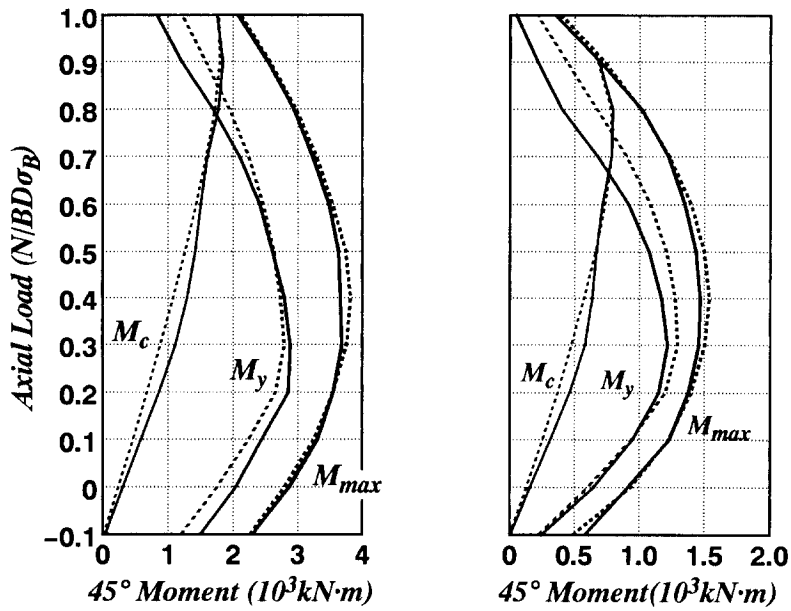


(a) S2(9-SS, 16-CS) (b) S3(8-SS, 16-CS)

Fig. 8 $N$-$M_c$, $N$-$M_y$, $N$-$M_{max}$ Curves of Sections S2, S3 by Proposed Model(Solid) and Integration Method (Dash)

Table 3 Material Properties of Column Specimens(mm², MPa)

| Specimen | | B8-2 | | | P3-C | | HB2 | |
|---|---|---|---|---|---|---|---|---|
| Steel Bar | Type | D6 | D10 | $\phi$4 | D10 | D25 | $\phi$5 | D13 |
| | Area | 32 | 71 | 13 | 71 | 507 | 20 | 127 |
| | $\sigma_{sy}$ | 386 | 417 | 482 | 324 | 362 | 980 | 637 |
| | $E_s(10^5)$ | – | 2.1 | – | 1.87 | 1.81 | – | 1.88 |
| Concrete | $K$ | 1.2 | | | 1.25 | | 1.25 | |
| | $\sigma_B$ | 30.7 | | | 27.5 | | 67.0 | |
| | $\varepsilon_B$ | 0.0022 | | | 0.002 | | 0.0026 | |
| | $\sigma_t$ | 2.65 | | | 2.6 | | 2.92 | |

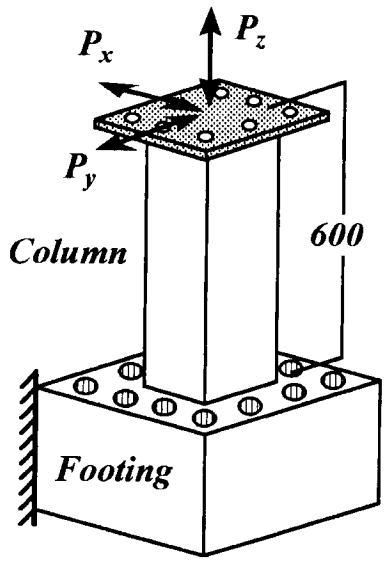


Specimens B8-2, P3-C

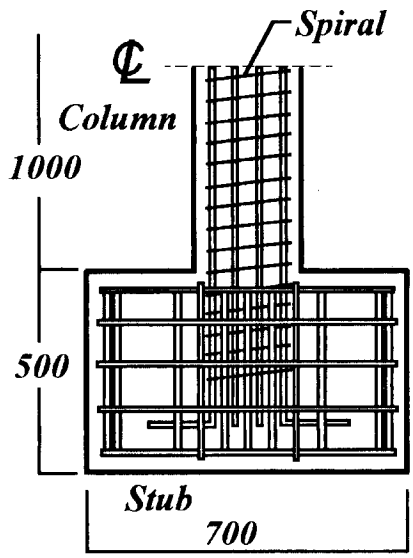


under Anti-symmetrical
Biaxial Bending and Axial Load

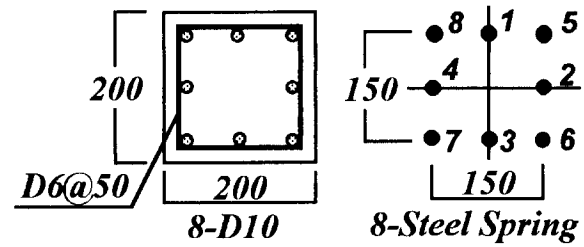


(a) B8-2($b=d=160$, $t_s=20$)

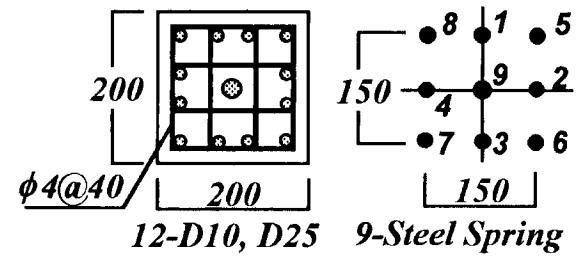


(b) P3-C($b=d=160$, $t_s=20$)

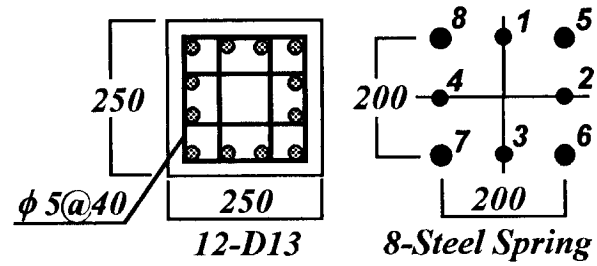


(c) HB2($b=d=200$, $t_s=25$)

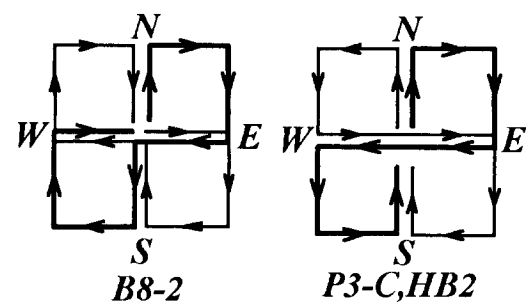


(d) Loading Path

Fig. 9 RC Column Test Specimens(Unit in mm)

Table 4 Multi-Spring Parameters for Column Specimens

| Specimen | | B8-2 | P3-C | HB2 |
|---|---|---|---|---|
| Model | | 8-SS, 16-CS | 9-SS, 16-CS | 8-SS, 16-CS |
| $\eta L_0$(mm) | | 100 | 100 | 125 |
| $\kappa$ | | 1.67 | 1.67 | 1.50 |
| SS | *1~4 | 29.7 | 30.8 | 108 |
| $f_{sy}$ | 5~8 | 29.7 | 38.5 | 135 |
| (kN) | 9 | | 184 | |
| $d_{sy}$(mm) | | 0.20 | 0.17 | 0.42 |
| CS | *1~8 | 118 | 110 | 419 |
| $f_{sy}$ | 9~12 | 49.2 | 44.0 | 168 |
| (kN) | 13~16 | 61.4 | 55.0 | 210 |
| $d_{cy}$ | *1~8 | 0.26 | 0.25 | 0.41 |
| (mm) | 9~16 | 0.22 | 0.20 | 0.33 |

* Spring Number

## 7. Comparison of model with RC column test data

Three columns were tested under axial load and bi-directional bending; i.e., specimen B8-2 (Li et al. 1987), specimen P3-C (Tatsumi et al. 1990), and specimens HB2 (Kabeyasawa 1991). The dimensions of the specimens are shown in Fig.9, and the material properties listed in Table 3. The parameters of the proposed model are listed in Table 4.

For the analysis of a specimen under load reversals, hysteresis rules are assumed for a concrete and steel spring as shown in Fig.10. A degrading unloading stiffness is used for both steel and concrete springs. The resistance of a concrete spring during unloading after maximum compression resistance and after tension cracking, shown in Fig.10(b) in steps, is kept constant at each step for numerical stability, and the error is corrected in the next loading step. All specimens showed predominantly flexural behavior, therefore, the shear stiffness is assumed to remain elastic in the analysis. The axial load and lateral displacements observed at the column top are used to calculate column moments and axial deformation.

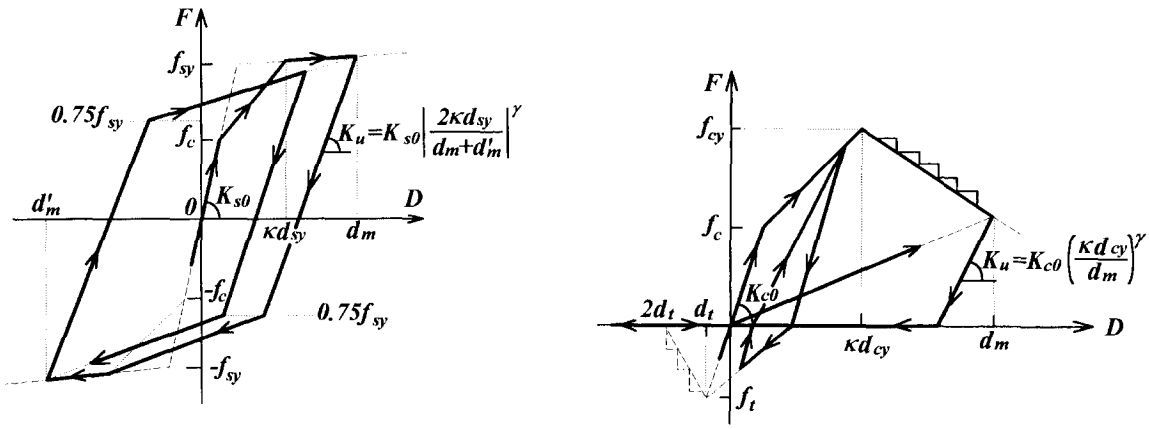


(a) Steel Spring (b) Concrete Spring

Fig. 10 Spring Hysteresis Rules

The axial load of specimen B8-2 was varied between -0.06 to 0.19 times $BD\sigma_B$, proportional to lateral resistances, while a constant axial load at $0.3BD\sigma_B$ was applied to specimen P3-C. The analysis results are comparable with the tested results as shown in Figs.11 and 12. The model can also reproduce the experimental results of high strength reinforced concrete columns. Specimens HB2 was tested under anti-symmetrical biaxial moments and a varying axial load between -0.1 and $0.6BD\sigma_B$. The calculated response by the model is compared with the observed response in Fig.13, in which a reasonable agreement can be observed.

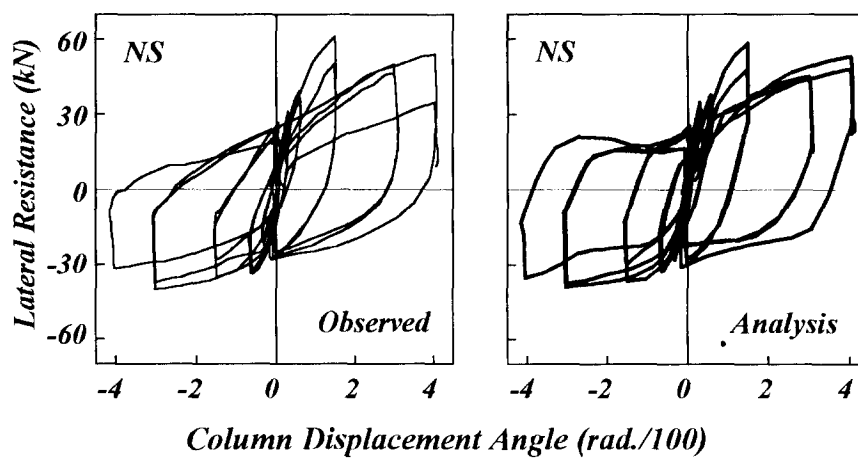


Fig. 11 Comparison of Analysis and Observed Results of B8-2

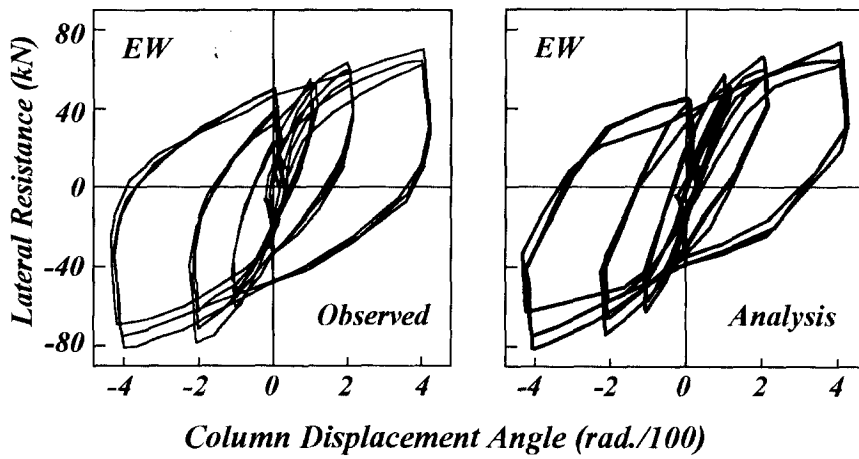


Fig. 12 Comparison of Analysis and Observed Results of P3-C

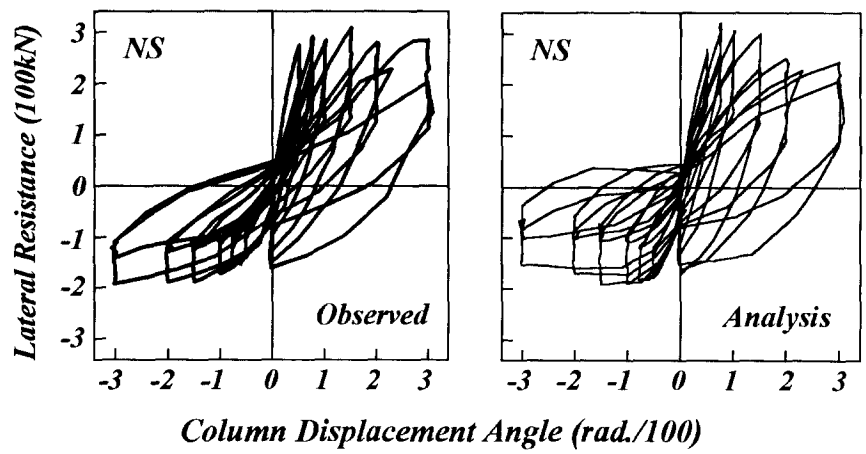


Fig. 13 Comparison of Analysis and Observed Results of High Strength RC Columns

The proposed model is implemented in Program CANNY for the analysis of a three-dimensional reinforced concrete frame structure under static and dynamic loading (Li 1992).

## 8. Conclusions

A multi-spring model is modified to increase the number of springs. The model is applicable to an RC member with arbitrary section shape. The reliability of the model is examined with respect to test data. The analysis results predicted by the model agreed well with the experimental results of both normal and high strength reinforced concrete columns under bi-directional bending reversals and varying axial loads.

## Acknowledgements

Authors thank Professor Toshimi Kabeyasawa of Yokohama National University, Japan, for permitting them to use his test results on reinforced concrete columns. The computation work and the preparation of the paper were done in Department of Civil Engineering at National University of Singapore.

## References

Fukuzawa, E., Isozaki, Y. and Fujisaki, K. (1988), "Elastic-Plastic Earthquake Response Analysis of Reinforced Concrete Frame in Consideration of Fluctuation of Axial Forces on Columns," *Procs., Ninth World Conference on Earthquake Eng.*, **8**, 549-554.

Giberson, M.F. (1967), "The Response of Nonlinear Multi-story Structures subjected to Earthquake Excitation," Earthquake Eng. Research Laboratory, California Institute of Technology.

Jiang, Y. and Saiidi, S.M. (1990), "Four-Spring Element for Cyclic Response of R/C Columns," *J., Struct. Eng., ASCE,* **116**(4), 1018-1029.

Kabeyasawa, T. and Shen, H. (1991), "Experimental Study on Behaviors of Ultrahigh Strength Reinforced Concrete Columns under Triaxial Forces," *Transactions, Japan Concrete Inst.*, **13**, 279-286.

Kent, D.C. and Park, R. (1971), "Flexural Members with Confined Concrete," *J., Struct. Eng. Division, ASCE,* **97**(7), 1969-1990.

Lai, S.-S., Will, G.T. and Otani, S. (1984), "Model for Inelastic Biaxial Bending of Concrete Member," *J., Struct. Eng., ASCE,* **110**(11), 2563-2584.

Li, K.-N., Otani, S. and Aoyama, H. (1987), "Reinforced Concrete Columns under Varying Axial Load and Bi-Direction Horizontal Load Reversals," *Proc., Pacific Conference on Earthquake Eng.*, Wairakei, New Zealand, **1**, Aug., 1987, 141-152.

Li, K.-N., Otani, S. and Aoyama, H. (1988), "Reinforced Concrete Columns Under Varying Axial Load and Bi-directional Lateral Load Reversals," *Procs., Ninth World Conference on Earthquake Eng.*, Tokyo-Kyoto, **VIII**, 537-542.

Li, K.-N., Otani, S. and Aoyama, H. (1989), "Nonlinear Earthquake Response of Reinforced Concrete Space Frames with Varying Axial Force," *Tansactions, Japan Concrete Inst.*, **11**, 247-254.

Li, K.-N. (1992), "CANNY - A General Purpose Computer Program for Calculating Nonlinear Static and Dynamic Response of 3-Dimensional Frame Structures Considering the Interaction among Varying Axial Load and Biaxial Bending Moments," *Research Report No. CE 003,* Dept. of Civil Eng., National Univ. of Singapore, Dec., 1992.

Otani, S., Kabeyasawa, T., Shiohara H. and Aoyama, H. (1985), "Analysis of the Full Scale Seven Story Reinforced Concrete Test Structure," *Earthquake Effects on Reinforced Concrete Structs. - U.S.-Japan Research, Pub., SP-84, ACI,* 203-240.

Park, R., Priestley, M.J.N. and Gill, W.D. (1982), "Ductility of Square-Confined Concrete Columns," *J., Struct. Eng., ASCE,* **108** (4), 929-950.

Takizawa, H. and Aoyama, H. (1976), "Biaxial Effects in Modeling Earthquake Response of R/C Structures," *Earthquake Eng. and Struct. Dynamics,* **4**, 523-552.

Tatsumi, Y., Otani, S. and Aoyama, H. (1990) "Behavior of Reinforced Concrete Columns under Bi-directional Lateral and Large Varying Axial Loads (in Japanese)," *J., Struct. Eng., Archit. Inst. of Japan,* **36B**, 211-218.